MFIE Analysis and Design of Ridged Waveguides

Weimin Sun, *Member, IEEE,* and Constantine A. Balanis, *Fellow, IEEE*

Abstract—**This paper presents a unified approach for the analysis and design of ridged waveguides by a magnetic field integral equation (MFIE) formulation. The MFIE approach allows accurate and complete solution via a simple numerical implementation of pulse basis functions. The emphasis of the paper is oriented to the design of ridged waveguides for applications in microwave components and systems, rather than to details of numerical algorithms. Erroneous bandwidth estimates due to neglect of the TE_{11} mode in previous works have been corrected; and various useful design curves on cutoff frequency, bandwidth, attenuation, and waveguide impedance are provided. The proposed theory is verified by comparison to exact closed-form solutions and other published results.**

I. Introduction

RIDGED waveguides have many applications in microwave and antenna systems because of their unique characteristics of low cutoff frequency, wide bandwidth, and low impedance compatible with coaxial cables. The research endlessly continues, as reported in the literature. In the early pioneering works, the transverse resonance technique [1]–[5] was primarily used to find the dominant cutoff frequencies and generate design curves. This method involved the approximation of the ridge step discontinuity susceptance and the assumption of simple transverse field distribution, which in turn limited the accuracy particularly when the waveguide has a narrow ridge thickness or narrow ridge gap. Moreover, the neglect of the TE_{11} mode led to erroneous bandwidth estimates for waveguides.

Later, more analyses [6]–[11] were performed by representing the transverse field as a sum of harmonic functions, and matching tangential fields on the aperture of the ridge edge. This technique is accurate in its nature, however, it is limited in use to rectangular waveguides with rectangular thick ridges. Among various analysis techniques, there are the variational method [12] and the spectral domain method [13], [14], which is very successful in dealing with fin-line loaded waveguides. These two methods also partly rely on the use of harmonic expansion functions for the transverse fields; thus, they are not flexible for treating arbitrarily shaped ridges.

In recent years, the surface integral equation approach has been proposed to solve propagation modes in waveguides with arbitrary cross sections [15]–[17]. It is demonstrated that the surface integral equation is robust in formulation and flexible for geometry modeling. In previous publications, the integral equation analyses were generic ones, not specific on ridged waveguides. Their subsequent numerical solutions were not thorough in the extent of meeting a normal design need. Furthermore, the proposed electric field integral equation (EFIE) has higher order derivative in the formulation, and its numerical counterpart is less efficient when compared to a magnetic field integral equation (MFIE) formulation.

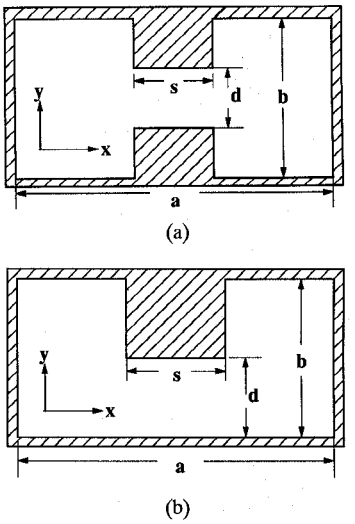

Fig. 1. Geometry of typical double-ridge (a) and single-ridged (b) waveguides.

As the application of ridged waveguide is increasing in microwave components and systems (such as a broadband filter, ortho-mode transducer, impedance transformer, and broadband microwave power feeding for either an antenna or amplifier), accurate analysis and design of a ridged waveguide are necessary.

In this paper, an MFIE technique is proposed to pursue precise and complete solutions to ridged waveguide modes, including cutoff frequency, bandwidth, attenuation, and waveguide impedance. The use of MFIE allows simple numerical implementation by using pulse basis functions, while it provides an improved numerical solution.

In Section II, an MFIE formulation is established and used to calculate cutoff frequencies and surface modal currents of both TE and TM modes. After, it is shown that the field distribution inside a ridged waveguide, its attenuation constant, and waveguide impedance are determined from the solution of the surface currents.

In Section III, standard ridgeless waveguides are first analyzed by the proposed theory to validate the formulation and compare the numerical accuracy. To provide basic design guidelines, several sets of parametric design curves are plotted to illustrate the dependence of cutoff wavelength, waveguide impedance, and attenuation constant on the ridge dimensions. Lastly, several field distribution patterns of dominant modes

Manuscript received July 13, 1992; revised February 17, 1993.

The authors are with the Telecommunications Research Center, Arizona State University, Tempe, AZ 85287-7206.

IEEE Log Number 9212730.

are drawn in contour plots to show insight into the waveguide modes.

II. Formulation

Based on equivalence principles, integral equations for both electric and magnetic fields can be derived [18], [19]. However, in a waveguide with a uniform cross section, only two-dimensional equations are necessary. On the inner surface of a perfectly conducting waveguide, such as a ridged waveguide as shown in Fig. 1, the magnetic field can be represented by the surface integral of the electric current density as

$$\boldsymbol{H}(\rho) = \frac{1}{2\pi} \oint_c \boldsymbol{J}(\rho') \times (\nabla_t' + j\beta_z \hat{z}) G \, dl' \tag{1}$$

where ρ is the position vector in two-dimensional space, $\oint_c$ is the circumferential contour integration, ∇_t is the transverse differential operator, β_z is the phase constant in the z direction, $\hat{z}$ is the unit vector in the z direction, and

$$G = \frac{\pi}{j} H_0^{(2)}\left(\sqrt{k^2 - \beta_z^2}|\rho - \rho'|\right) \tag{2}$$

with $H_0^{(2)}$ being the Hankel function of the second kind, $\boldsymbol{J}$ the electric surface current density, and k the wavenumber in free space.

It is worthwhile to point out that since (1) models an arbitrarily shaped waveguide, the following solution procedure applies to waveguides with an arbitrary uniform cross section and multiple ridges. Indeed, (1) is the formulation that can be used to solve quadruple-ridged waveguides. The analysis on the quadruple-ridged waveguides will be presented in a later paper.

A. Determination of Cutoff Frequency

It can be shown that the MFIE of (1) is sufficient to determine the cutoff frequencies of both TE and TM modes for a ridged waveguide. At cutoff, $k = k_c$, $\beta_z = 0$; therefore, (1) leads to

$$2\pi \boldsymbol{H}(\rho) = \oint_c \boldsymbol{J}(\rho') \times \nabla_t' G \, dl' \tag{3}$$

or

$$2\pi \hat{n} \times \boldsymbol{J}(\rho) + \oint_c \boldsymbol{J}(\rho') \times \nabla_t' G \, dl' = 0 \tag{4}$$

on the waveguide inner surface with a normal direction of $\hat{n}$. The circumferential and axial components of (4), respectively, are

$$2\pi J_z(\rho) + \oint_c J_z(\rho') \hat{t} \cdot (\hat{z} \times \nabla_t') G \, dl' = 0 \tag{5}$$

$$-2\pi J_t(\rho) + \oint_c J_t(\rho') \hat{z} \cdot (\hat{t} \times \nabla_t') G \, dl' = 0 \tag{6}$$

where $\hat{t}$ is a unit vector in the tangential direction of the waveguide wall.

Completing the vector manipulation, explicit integral equations of the circumferential and the axial surface current densities are obtained at cutoff as

$$2J_z(\rho) - jk_c \oint_c J_z(\rho') \sin\left(\hat{t}, \frac{\rho' - \rho}{|\rho - \rho'|}\right) \cdot H_1^{(2)}(k_c|\rho - \rho'|) \, dl' = 0 \tag{7}$$

$$2J_t(\rho) - jk_c \oint_c J_t(\rho') \sin\left(\hat{t}', \frac{\rho' - \rho}{|\rho - \rho'|}\right) \cdot H_1^{(2)}(k_c|\rho - \rho'|) \, dl' = 0. \tag{8}$$

In (7) and (8), the $\sin(\boldsymbol{a}, \boldsymbol{b})$ represents the sine function of the angle between two unit vectors $\boldsymbol{a}$ and $\boldsymbol{b}$. Equations (7) and (8) are fundamental to determine the cutoff frequencies of both TE and TM modes. Since, at cutoff, a TE mode only supports circumferential surface current density, and a TM mode only supports longitudinal current density, then either (7) or (8) is required to determine the cutoff frequency of a TE or a TM mode.

TABLE I
Normalized Cutoff Wavenumber $k_c a$ of a Rectangular Waveguide ($b = 0.5a$)

Mode	$k_c a$	
	exact	MFIE
TE_{10}	3.14159	3.14828
TE_{11}	7.02481	7.02475
TE_{12}	12.9531	12.9583
TE_{13}	19.1096	19.1099
TE_{20}	6.28319	6.28733
TE_{21}	8.88577	8.89259
TE_{22}	14.0496	14.0546
TE_{23}	19.8692	19.8683
TE_{30}	9.42478	9.42747
TE_{31}	11.3272	11.3345
TE_{32}	15.7080	15.7049
TE_{40}	12.5664	12.5673
TE_{41}	14.0496	14.0532
TE_{42}	17.7715	17.7761
TE_{50}	15.7080	15.7049
TE_{51}	16.9180	16.9209
TE_{52}	20.1160	20.1206
TE_{60}	18.8496	18.8507
TE_{61}	19.8692	19.8683

TABLE II
Normalized Cutoff Wavenumber $k_c a$ of a Circular Waveguide

Mode	$k_c a$			Mode	$k_c a$		
TE_{mn}	Ref. [21]	MFIE	Ref. [15]	TM_{mn}	Ref. [21]	MFIE	Ref. [15]
TE_{11}	1.84118	1.84202	1.8462	TM_{01}	2.40482	2.40530	2.4111
TE_{21}	3.05424	3.05510	3.0645	TM_{11}	3.83171	3.83218	3.8416
TE_{31}	4.20119	4.20171	4.2200	TM_{21}	5.13562	5.13616	5.1485
TE_{41}	5.31755	5.31851		TM_{31}	6.38016	6.38076	
TE_{51}	6.41562	6.41689		TM_{41}	7.58834	7.58901	
TE_{61}	7.50127	7.50233		TM_{51}	8.77148	8.77221	
TE_{71}	8.57784	8.53716		TM_{61}	9.93611	9.93691	
TE_{81}	9.64742	9.64862		TM_{71}	11.0864	11.0872	
TE_{02}	3.83170	3.83214	3.8422	TM_{02}	5.52007	5.52055	5.5346
TE_{12}	5.33144	5.33206		TM_{12}	7.01559	7.01613	
TE_{22}	6.70613	6.70666		TM_{22}	8.41724	8.41787	
TE_{32}	8.01524	8.01577		TM_{42}	11.0647	11.0655	
TE_{42}	9.28240	9.28304		TM_{52}	12.3386	12.3394	
TE_{52}	10.5199	10.5201		TM_{03}	8.65372	8.65433	
TE_{62}	11 7349	11.7358		TM_{13}	10.1735	10.1742	
TE_{03}	7.01588	7.01609		TM_{04}	11.7915	11.7923	
TE_{13}	8.53632	8.53702		TM_{14}	13.3237	13.3246	
TE_{33}	11.3459	11.3466		TM_{24}	14.7960	14.7969	
TE_{14}	11.7060	10.7067					
TE_{24}	13.1704	13.1711					

B. Solution of Modal Current

Once the cutoff frequency of a waveguide mode is determined, the modal surface current can be obtained from the solution of (1), if the magnetic field $\boldsymbol{H}$ on the left-hand side of (1) is replaced by the surface current $\hat{n} \times \boldsymbol{J}$, and (1) is decomposed into $\hat{t}$ and $\hat{z}$ components as

$$2J_t(\rho) - \oint_c J_t(\rho') \sin\left(\hat{t}', \frac{\rho' - \rho}{|\rho - \rho'|}\right) \cdot H_1^{(2)}(k_c|\rho - \rho'|)\, dl' = 0 \tag{9}$$

and

$$2J_z(\rho) - jk_c \oint_c J_z(\rho') \sin\left(\hat{t}, \frac{\rho' - \rho}{|\rho - \rho'|}\right) H_1^{(2)}(k_c|\rho - \rho'|)\, dl' + \beta_z \oint_c J_t(\rho') \cos(\hat{t}, \hat{n}') H_0^{(2)}(k_c|\rho - \rho'|)\, dl' = 0. \tag{10}$$

For a TE mode, when the operation frequency is above cutoff, both the $\hat{t}$ and $\hat{z}$ components of surface current density will be excited. Equation (9) is used to obtain solution of J_t first, and (10) is subsequently used to determine J_z. However, for a TM mode, only (10) is necessary to obtain solution of J_z because J_t vanishes in a TM mode.

C. Electric and Magnetic Field

When the surface current is determined, the magnetic field inside the waveguide can be obtained from (1) via a simple integration. Decomposing (1) into its rectangular components, it can be written as

$$H_x = \frac{1}{4} \oint_c \left[t_y' \beta_z J_t H_0(k_c R) + jk_c J_z \frac{\Delta y}{R} H_1(k_c R) \right] dl' \tag{11}$$

$$H_y = -\frac{1}{4} \oint_c \left[t_x' \beta_z J_t H_0(k_c R) + jk_c J_z \frac{\Delta x}{R} H_1(k_c R) \right] dl' \tag{12}$$

$$H_z = -\frac{jk_c}{4} \oint_c J_t \hat{z} \cdot \left(\hat{t}' \times \frac{\boldsymbol{R}}{R} \right) H_1(k_c R)\, dl' \tag{13}$$

where t_y' and t_x' are the x- and y-components of the unit vector $\hat{t}'$, $\Delta x = x - x'$, $\Delta y = y - y'$, and $R = |\rho - \rho'|$.

In most applications, only the transverse electric field is of interest. However, inside a conducting waveguide, the transverse electric field is linearly proportional to the transverse magnetic field. From general waveguide theory, the transverse electric and magnetic field components can be expressed in terms of the longitudinal components as

$$TE \text{ Mode} \begin{cases} \boldsymbol{H}_t = -j\beta_z / k_c^2 \nabla_t H_z \\ \boldsymbol{E}_t = -\omega\mu / \beta_z \hat{z} \times \boldsymbol{H}_t \end{cases} \tag{14}$$

$$TM \text{ Mode} \begin{cases} \boldsymbol{E}_t = -j\beta_z / k_c^2 \nabla_t E_z \\ \boldsymbol{H}_t = -\omega\epsilon / \beta_z \hat{z} \times \boldsymbol{E}_t \end{cases} \tag{15}$$

Thus, the transverse electric fields are related to the transverse magnetic fields by

$$TE \text{ Mode} \begin{cases} E_x = \omega\mu / \beta z H_y \\ E_y = -\omega\mu / \beta_z H_x \end{cases} \tag{16}$$

$$TM \text{ Mode} \begin{cases} E_x = \beta_z / \omega\epsilon H_y \\ E_y = -\beta_z / \omega\epsilon H_x \end{cases} \tag{17}$$

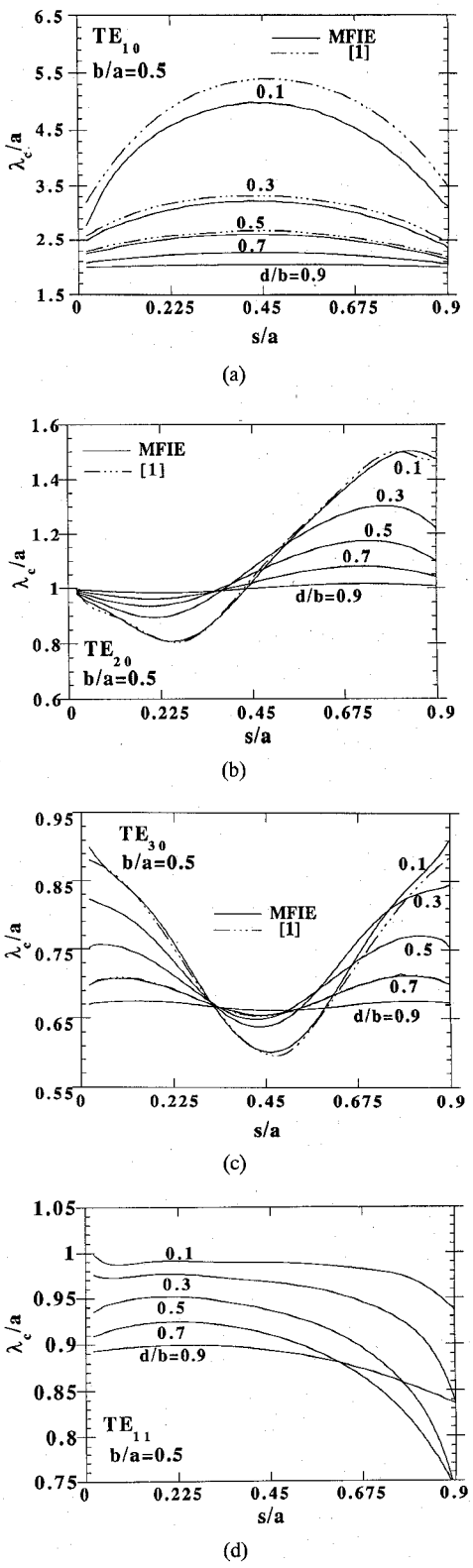

Fig. 2. Normalized TE mode cutoff wavelength of a double-ridged waveguide with aspect ratio $b/a = 0.5$. (a) TE_{10}, (b) TE_{20}, (c) TE_{30}, (d) TE_{11}.

D. Power Attenuation and Waveguide Impedance

In the design of a ridged waveguide component or system, it is informative to know its power attenuation constant and waveguide impedance. In previous works, analyses on the attenuation and the impedance of a ridged waveguide were

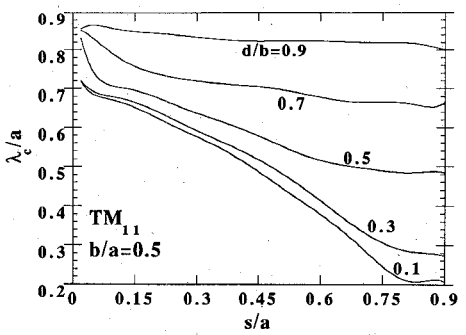

Fig. 3. Normalized TM_{11} mode cutoff wavelength of a double-ridged waveguide with aspect ratio $b/a = 0.5$.

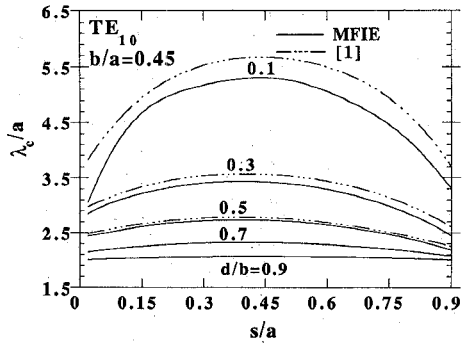

(a)

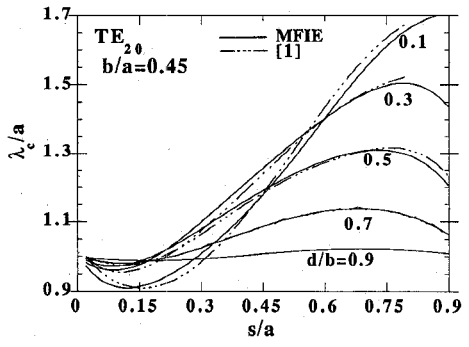

(b)

Fig. 4. Normalized TE mode cutoff wavelength of a single-ridged waveguide with aspect ratio $b/a = 0.45$. (a) TE_{10}, (b) TE_{20}.

not accurate and sufficient for use in waveguide design. With the powerful and versatile MFIE formulation, it is convenient to obtain accurate attenuation constants and waveguide impedances.

The attenuation constant α is defined by

$$\alpha = \frac{P_c}{2P} \tag{18}$$

where

$$P_c = \frac{R_s}{2} \oint_c |J|^2 \, dl \tag{19}$$

is the surface conducting loss with surface resistance R_s per unit square, and

$$P = \frac{1}{2} \operatorname{Re} \int_s \boldsymbol{E} \times \boldsymbol{H}^* \cdot d\boldsymbol{s} \tag{20}$$

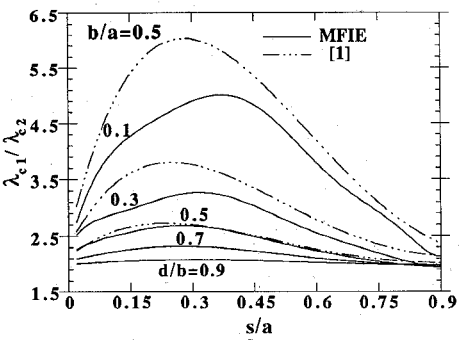

(a)

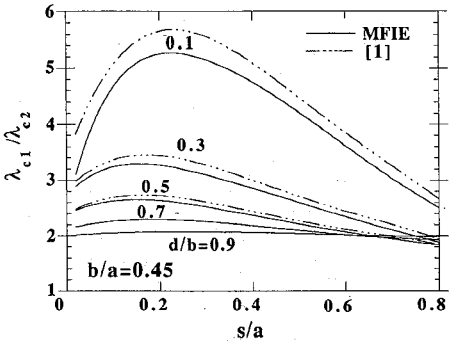

(b)

Fig. 5. Frequency bandwidth of a ridged waveguide (λ_{c1} cutoff wavelength of the first dominant mode and λ_{c2} cutoff wavelength of the second dominant mode). (a) Double ridged, (b) single ridged.

is the power flux in the waveguide. It is a common practice to define the waveguide impedance from a power consideration as

$$Z_{pv} = \frac{V_0^2}{2P}. \tag{21}$$

The same definition was also used in [1], [7], [9], [12], and [14]. In (21), V_0 is the peak voltage across the ridge gap, and can be evaluated by the integral

$$V_0 = \int_y E_y \, dl. \tag{22}$$

Once the modal surface current density is known, the tangential magnetic fields are obtained via (11)–(13), and in turn the waveguide impedance and attenuation via (23) and (24).

III. Numerial Results

A simple numerical scheme utilizing pulse basis functions and delta weighting functions is used in a Method of Moment (MoM) [20] numerical solution. Following the established theory and its numerical procedure, many numerical results and design curves have been obtained. For brevity, only partial results of ridged waveguides with typical aspect ratios are presented here.

To validate the formulation and verify the accuracy of the proposed method, the procedure was first applied to ridgeless waveguides, rectangular and circular, with known exact solutions. The computed cutoff wavenumbers are listed in Tables I and II, and are compared to exact closed-form

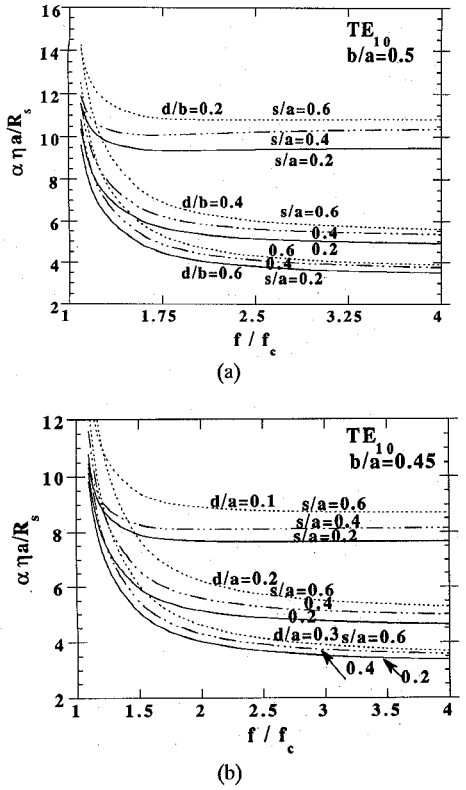

Fig. 6. Normalized attenuation constant of a ridged waveguide (f_c cutoff frequency of TE_{10} mode). (a) Double ridged, (b) single ridged.

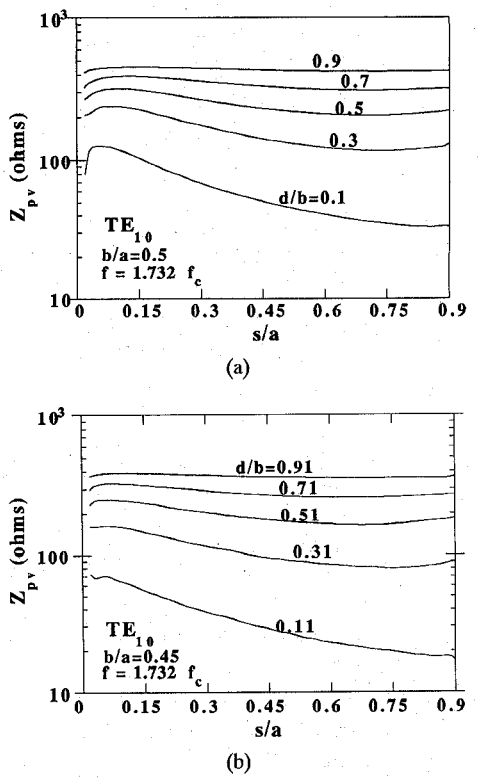

Fig. 7. TE_{10} mode waveguide impedance of a ridged waveguide (f_c cutoff frequency of TE_{10} mode). (a) Double ridged, (b) single ridged.

solutions [21]. It is observed that the computed normalized cutoff wavenumbers of rectangular and circular waveguides agree with the exact values up to 4 digits. However, those of [15] in Table II, via an EFIE formulation, agree only up to 2 and 3 digits. This comparison presumes that the same number of basis functions is used.

A. Cutoff Wavelength and Bandwidth

Since the ridged waveguides are used mostly to achieve larger bandwidths, it is of interest to estimate the bandwidth. The bandwidth defines the frequency range in which the waveguide only supports one propagation mode. Because the second lowest mode in a rectangular waveguide with aspect ratio $b/a < 0.5$ is the TE_{20} mode, the hybrid TE_{20} mode in a ridged waveguide was assumed to be the second lowest in all of previous works. Unfortunately, this is not always the case. In fact, the TE_{11} may become the second lowest when the ridge gap is narrow. It should be pointed out that the TE_{11} mode in this paper is the same as the TE_{10} trough mode in [7], since the TE_{10} trough mode is a transition form the TE_{11} mode in a ridgeless rectangular waveguide.

In Fig. 2(a)–(d), the normalized cutoff wavelength of a double-ridged waveguide with an aspect ratio $b/a = 0.5$, shown in Fig. 1, is plotted versus the geometry of the ridge. The wavelength and the waveguide dimensions are normalized with respect to the waveguide width a. The dashed lines in Fig. 2 represent the data by Hopfer [1]. It is apparent from the data of Fig. 2 that the current theory is fairly consistent with [1] of the transverse resonance approach on dominant cutoff wavelengths. The cutoff wavelength of the TM_{11} mode for the

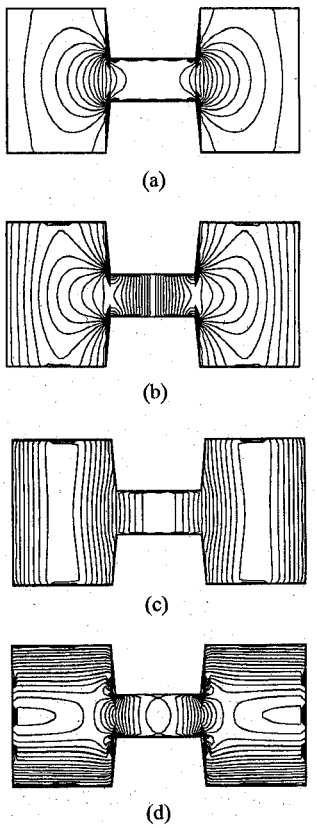

Fig. 8. Electrical field contour plots of a double-ridged waveguide (ridge thickness $s/a = 0.3$ and ridge gap $d/a = 0.15$). (a) TE_{10}, (b) TE_{20}, (c) TE_{30}, and (d) TE_{11} modes.

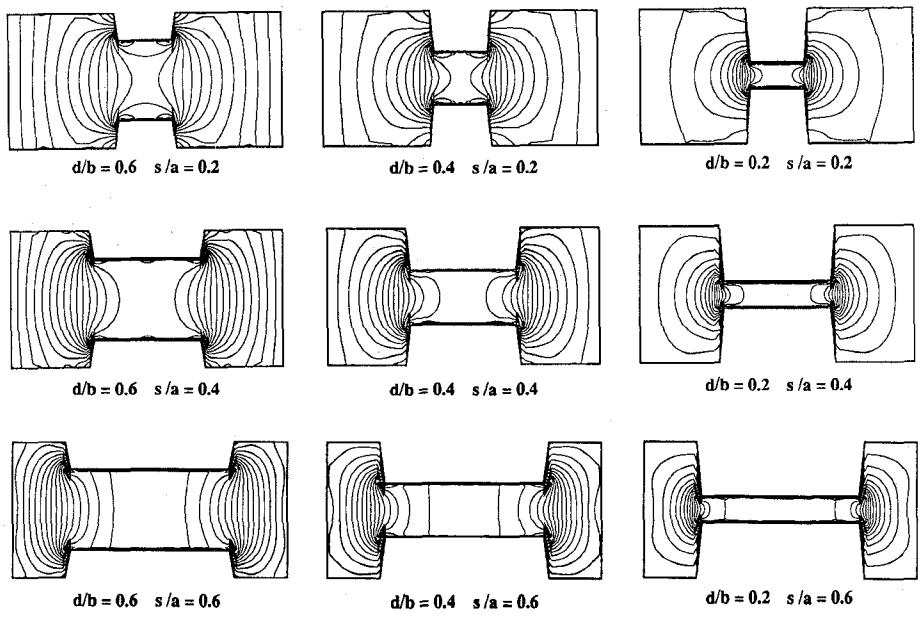

Fig. 9. Electric field contour plots of TE_{10} mode in double-ridged waveguides with various s/a and d/b ratios.

same double-ridged waveguide is given in Fig. 3 to illustrate that the TM mode has a shorter cutoff wavelength and is less dominant than a TE mode. Fig. 4(a)–(b) shows the dominant cutoff wavelength of a single-ridged waveguide with aspect ratio $b/a = 0.45$, where only the TE_{10} and TE_{20} modes are presented. The available results of [1] are also compared, although the curves of the TE_{20} mode were incomplete in [1].

It is found that in the case of double-ridged waveguide of $b/a = 0.5$, the TE_{11} may become the second lowest mode when the ridge gap d is less than 20 percent of the waveguide width a and the ridge thickness s is less than 35 percent of a. However, in the case of single-ridged waveguide with aspect ratio $b/a = 0.45$, the TE_{11} has a higher cutoff frequency than the TE_{20}. Bandwidth curves are shown in Fig. 5(a) and (b) for double- and single-ridged guides, respectively.

B. Attenuation and Impedance

In various ridged waveguide component or antenna feed designs, knowledge of waveguide attenuation and waveguide impedance is necessary. The waveguide attenuation constant is shown in Fig. 6(a) and (b), where the attenuation constant α defined in (20) is normalized with R_s (wall surface resistance per unit square), η (free space wave impedance), and a (waveguide width). It is evident that smaller ridge gaps or larger thicknesses lead to larger attenuation.

The waveguide impedance defined in (21) for both double- and single-ridged waveguides is first computed at a fixed frequency, by varying the ridge dimensions. Fig. 7(a) shows the impedance of a double-ridged waveguide. The operation frequency is fixed at $\sqrt{3}$ times of the TE_{10} cutoff frequency. The impedance can be substantially low if the ridge gap is very narrow. Fig. 7(b) is the impedance of a single-ridged waveguide at the same reference frequency.

C. Field Distribution

The task to pursue the solution of modal field distribution at different frequencies with different ridge parameters is certainly vast. Limited by the size of this paper, only a few typical modal field patterns are presented here. The contour plot technique is used to draw contour electric field lines, as shown in Fig. 9(a)–(c), in which the center of the contours represents the location of peak E-fields and dense lines represent rapid variations of E-fields.

The E-field contours of the TE_{10}, TE_{20}, TE_{30}, and TE_{11} modes in a double-ridged guide are shown in Fig. (a)–(d) where the ridge gap d and thickness s are 15 and 30 percent, respectively, of the waveguide width a. The electric field of the TE_{10} is very concentrated between ridge gaps, while the electric field of the TE_{30} mode is distributed in two cavities. It is also seen that TE_{11} is a trough mode. In order to see the effect of the s/a and d/b ratios on the field patterns, Fig. 9 is provided to show the field distributions of TE_{10} mode in various double-ridged waveguides.

IV. Conclusion

The surface magnetic field integral equation is used to analyze ridged waveguides in an efficient way. The formulation is flexible in handling various waveguide cross sections and ridge shapes, and accurate in determining waveguide modes; and it remains simple in numerical solution with pulse basis functions.

In a double-ridged waveguide, the second lowest mode may not be the TE_{20} mode, as taken for granted previously, and the bandwidth is estimated to be smaller in a waveguide with narrow ridge gap, compared to existing results.

The ridged waveguide attenuation is proportional to the ridge thickness, and inversely proportional to the ridge gap. When the ridge gap d/b is less than 0.2 and the frequency is well above cutoff ($f \geq 1.73fc$), the attenuation increases only slightly with frequency. However, the waveguide impedance is proportional to the ridge gap, and inversely proportional to the ridge thickness. A low impedance, which is compatible with a coaxial cable, can be achieved by decreasing the ridge gap d/b to less than 0.1. Unfortunately, a low impedance is

always coupled with a high attenuation, and a tradeoff has to be considered in design practice.

The multiridged and arbitrarily shaped waveguides can be analyzed by the same technique. The formulation and numerical results on general types of quadruple-ridged waveguides (such as square, diagonal, and circular waveguides) will be presented in a later publication.

REFERENCES

[1] S. Hopfer, "The design of ridged waveguide," *IRE Trans. Microwave Theory Tech.*, vol. MTT-3, pp. 20–29, Oct. 1955.

[2] N. Marcuvitz, *Waveguide Handbook*, M.I.T. Rad. Lab. Series, vol. 10. New York: McGraw Hill, 1951, pp. 399–402.

[3] S. B. Cohn, "Properties of ridge waveguide," *Proc. IRE*, vol. 35, pp. 783–788, Aug. 1947.

[4] T. S. Chen, "Calculation of the parameters of ridge waveguides," *IRE Trans. Microwave Theory Tech.*, vol. MTT-5, pp. 12–17, Jan. 1957.

[5] J. R. Pyle, "The cutoff wavelength of the TE_{10} mode in ridged rectangular waveguide of any aspect ratio," *IEEE Trans. Microwave Theory Tech.*, vol. MTT-14, pp. 175–183, Apr. 1966.

[6] W. J. Getsinger, "Ridge waveguide field description and application to directional coupler," *IRE Trans. Microwave Theory Tech.*, vol. MTT-10, pp. 41–50, Jan. 1962.

[7] J. R. Montgomery, "On the complete eigenvalue solution of ridged waveguide," *IEEE Trans. Microwave Theory Tech.*, vol. MTT-19, pp. 547–555, June 1971.

[8] D. Dasgupta and P. K. Saha, "Eigenvalue spectrum of rectangular waveguide with two symmetrically placed double ridges," *IEEE Trans. Microwave Theory Tech.*, vol. MTT-29, pp. 47–51, Jan. 1981.

[9] ——, "Rectangular waveguide with two double ridges," *IEEE Trans. Microwave Theory Tech.*, vol. MTT-31, pp. 938–941, Nov. 1983.

[10] G. G. Mazumder and P. K. Saha, "A novel rectangular waveguide with double T-septums," *IEEE Trans. Microwave Theory Tech.*, vol. MTT-33, pp. 1235–1238, Nov. 1985.

[11] J. Bornemann and F. Arndt, "Modal-s-matrix design of optimum stepped ridged and finned waveguide transformers," *IEEE Trans. Microwave Theory Tech.*, vol. MTT-35, pp. 561–567, June 1987.

[12] Y. Utsumi, "Variational analysis of ridged waveguide modes," *IEEE Trans. Microwave Theory Tech.*, vol. MTT-33, pp. 111–120, Feb. 1985.

[13] L. P. Schmidt and T. Itoh, "Spectral domain analysis of dominant and higher order modes in fin-lines," *IEEE Trans. Microwave Theory Tech.*, vol. MTT-28, pp. 981–985, Sept. 1980.

[14] T. Kitazawa and R. Mittra, "Analysis of finline with finite metallization thickness," *IEEE Trans. Microwave Theory Tech.*, vol. MTT-32, pp. 1484–1487, Nov. 1984.

[15] M. Swaminathan, E. Arvas, T. K. Sarkar, and A. R. Djordjevic, "Computation of cutoff wavenumbers of TE and TM modes in waveguides of arbitrary cross sections using a surface integral formulation," *IEEE Trans. Microwave Theory Tech.*, vol. MTT-38, pp. 154–159, Feb. 1990.

[16] C. Y. Kim, S. D. Yu, R. F. Harrington, J. W. Ra, and S. Y. Lee, "Computation of waveguide modes for waveguides of arbitrary cross-section," *IEE Proc.*, vol. 137, pt. H, pp. 145–149, Apr. 1990.

[17] M. Swaminathan, T. K. Sarkar, and A. T. Adams, "Computation of TM and TE modes in waveguides based on a surface integral formulation," *IEEE Trans. Microwave Theory Tech.*, vol. MTT-40, pp. 285–296, Feb. 1992.

[18] K. M. Chen, "A mathematical formulation of the equivalence principle," *IEEE Trans. Microwave Theory Tech.*, vol. MTT-37, pp. 1576–1581, Oct. 1989.

[19] X. Y. Min, W. M. Sun, W. Gesang, and K. M. Chen, "An efficient formulation to determine the scattering characteristics of a conducting body with thin magnetic coatings," *IEEE Trans. Antennas Propgat.*, vol. AP-39, pp. 448–454, Apr. 1991.

[20] R. F. Harrington, *Field Computations by Moment Methods*. New York: Macmillan, 1968.

[21] M. Abramowitz and I. A. Stegun, *Handbook of Mathematical Functions*. New York: Dover, 1965.

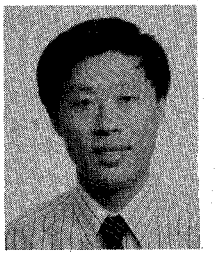

Weimin Sun (S'87–M'89) was born in Jiangsu province, China, in 1957. He received the B.S.E.E. degree in 1982 from Sichuan University, China; the M.S. degree in physical electronics in 1984 from Tsinghua University, China; and the Ph.D. degree in electrical engineering from Michigan State University, East Lansing, in 1989.

During his Ph.D. program, he was engaged in research including radar target discrimination with transient waveforms and interaction of electromagnetic waves with composite materials. From 1989 to 1991 he was an RF Research Engineer at MM-Wave Technology, Inc., where he designed and developed an 18–110 GHz millimeter-wave direction finding system. In 1992 he joined the Telecommunications Research Center of Arizona State University as an Assistant Research Engineer. His current research interests include computational electromagnetics, antenna measurement and design, and applications of advanced numerical techniques.

Dr. Sun is a member of Phi Kappa Phi. He was the recipient of the Outstanding Academic Award from the College of Engineering, Michigan State University, in 1988.

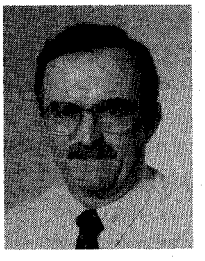

Constantine A. Balanis (S'62–M'68–SM'74–F'86) was born in Trikala, Greece. He received the B.S.E.E. degree from Virginia Tech, Blacksburg, in 1964; the M.E.E. degree from the University of Virginia, Charlottesville, in 1966; and the Ph.D. degree in electrical engineering from Ohio State University, Columbus, in 1969.

From 1964 to 1970 he was with NASA Langley Research Center, Hampton, VA; and from 1970 to 1983 he was with the Department of Electrical Engineering, West Virginia University, Morgantown. Since 1983 he has been with the Department of Electrical Engineering, Arizona State University, Tempe, where he is now Regents' Professor and Director of the Telecommunications Research Center. His research interests are in low- and high-frequency antenna and scattering methods, transient analysis and coupling of high-speed high-density integrated circuits, and multipath propagation. He received the 1992 Special Professionalism Award from the IEEE Phoenix Section, the 1989 IEEE Region 6 Individual Achievement Award, and the 1987–1988 Graduate Teaching Excellence Award, School of Engineering, Arizona State University. He is the author of *Antenna Theory: Analysis and Design* (New York: Wiley, 1982) and *Advanced Engineering Electromagnetics* (New York: Wiley, 1989).

Dr. Balanis is a member of ASEE, Sigma Xi, Electromagnetics Academy, Tau Beta Pi, Eta Kappa Nu, and Phi Kappa Phi. He has served as Associate Editor of the IEEE TRANSACTIONS ON ANTENNAS AND PROPAGATION (1974–1977) and the IEEE TRANSACTIONS ON GEOSCIENCE AND REMOTE SENSING (1981–1984), as Editor of the NEWSLETTER for the IEEE Geoscience and Remote Sensing Society (1982–1983), as Second Vice-President of the IEEE Geoscience and Remote Sensing Society (1984), and as Chairman of the Distinguished Lecturer Program of the IEEE Antennas and Propagation Society (1988–1991).